



Published in final edited form as:

Bone. 2007 February ; 40(2): 433–443.

Quantitative Trait Loci Modulate Vertebral Morphology and Mechanical Properties in a Population of 18 Month Old Genetically Heterogeneous Mice

Grant M. Reeves⁽¹⁾, Barbara R. McCreadie⁽¹⁾, Shu Chen⁽²⁾, Andrzej T. Galecki⁽²⁾, David T. Burke^{(2),(3)}, Richard A. Miller^{(2),(4)}, and Steven A. Goldstein^{(1),(2)}

(1) *Orthopaedic Research Laboratories, Department of Orthopaedic Surgery, University of Michigan, Ann Arbor, Michigan, USA*

(2) *Institute of Gerontology, University of Michigan, Ann Arbor, Michigan, USA*

(3) *Department of Human Genetics, University of Michigan, Ann Arbor, Michigan, USA*

(4) *Department of Pathology, Geriatrics Center, Ann Arbor VA Medical Center, University of Michigan, Ann Arbor, Michigan, USA*

Abstract

The aim of this study was to examine effects of polymorphic genes on vertebral bone morphology and mechanical properties. Genotypes from 525, 18 month old female mice were compared to geometric traits obtained from micro-computed tomography and mechanical properties from compression testing. Genetic markers were associated with traits on at least 13 different chromosomes, demonstrating the complexity of genetic control over vertebral form, function and aging.

Keywords

Quantitative trait loci; genetics; mice; mechanical properties; geometry

Introduction

Osteoporosis and age-related bone fragility are devastating conditions, resulting in more than 1.5 million fractures annually in the USA [1]. Vertebral fracture, a common result of osteoporosis, often leads to a characteristic hunched posture (thoracic kyphosis) and loss of height, and is associated with significant reduction in the quality of life [2]. It has been estimated that the average 50-year-old white woman has a 15.6% chance of vertebral fracture during her lifetime [1]. While it is well documented that osteoporosis victims have significantly altered morphologic and mechanical bone properties [3], the genetic factors that contribute to these properties are poorly understood.

Recent studies have begun to investigate genetic influences on bone properties. Since bone mineral density (BMD) is the current standard metric for the diagnosis of osteoporosis, many

Corresponding Author: Steven A. Goldstein, PhD, Orthopaedic Research Laboratories, University of Michigan, 2001 BSRB, 109 Zina Pitcher Place, Ann Arbor, MI 48109-2200. stevegl@umich.edu; (tel); 734-936-7417; (fax); 734-647-0003.

Publisher's Disclaimer: This is a PDF file of an unedited manuscript that has been accepted for publication. As a service to our customers we are providing this early version of the manuscript. The manuscript will undergo copyediting, typesetting, and review of the resulting proof before it is published in its final citable form. Please note that during the production process errors may be discovered which could affect the content, and all legal disclaimers that apply to the journal pertain.

genetic investigations have explored quantitative trait loci (QTL) that are associated with changes in BMD in humans and mice [e.g. 4-12]. However, BMD is only one of many properties of bones that contribute to their propensity to fracture [13]. Current perspectives on osteoporosis consider the risk of fracture to be related to both bone quantity (as measured by BMD) and bone quality [e.g.14,15]. While the specific metrics for quantifying bone quality remain under debate, understanding the genetics that regulate bone properties will provide insight that cannot be gained from BMD studies alone.

Several studies have focused on the identification of QTL that are associated with differences in bone morphologic and mechanical properties. QTL associated with morphologic and mechanical properties of murine femora [16,17], and morphologic properties of murine vertebrae at four months of age [18] have been identified. The purpose of this study was to investigate quantitative trait loci that affect the morphologic properties of vertebrae in aged mice. Furthermore, this study also sought to compare data collected from femurs from the same mice [16,17], to document differences or similarities in genetic control between the axial and appendicular skeleton.

Materials and Methods

Animals and Husbandry

The mice in this study were previously used to examine genetic effects on geometric and mechanical traits of femoral cortical bone [16,17]. UM-HET3 stock was derived from a four-way breeding among four inbred strains. The experimental animals are the female progeny of (BALB/cJ × C57BL/6J) F1 females and (C3H/HeJ × DBA/2J) F1 males. F1 breeding animals were purchased from Jackson Laboratories (Bar Harbor, ME, USA) and were used to produce a total of 525 UM-HET3 mice. Animals were housed by sex in a single suite of specific-pathogen-free (SPF) rooms and were exposed to controlled environmental conditions (12:12-h light/dark cycle, 23°C). Mice were given *ad libitum* access to water and laboratory mouse chow. The cages were covered with microisolator tops to minimize the spread of infectious agents. Sentinel mice were tested every 3 months to verify the pathogen-free status of the population. All such tests were negative throughout the course of the study. UM-HET3 female mice were entered into the study in a staggered fashion at a rate of 25-35 mice/month. It is important to note that no parental or grandparental genotypes (even at a single locus) are recapitulated in the UM-HET3 population studied. Consequently, only phenotypic comparisons within the 4-way cross population are genetically appropriate and were evaluated for this study. Animals were euthanized at 18 months of age. Eighth caudal vertebrae were removed, dissected free of soft tissue, and frozen in a phosphate-buffered saline solution. The 8th caudal vertebrae were chosen to represent an axial skeletal structure with sufficient trabecular bone and relatively parallel endplates perpendicular to the long axis of the bone. This work was approved by the University Committee on Use and Care of Animals at the University of Michigan.

Genotyping

As previously detailed by our group [16], genomic DNA was prepared from 1-cm sections of tail from 4-week-old animals and genotyped. In total, 185 markers were examined from 99 genetic loci. Of the 99 loci, 86 markers were informative for both the maternal- and paternal-derived alleles, and 13 loci were only informative for either maternal or paternal alleles. The selection of genetic loci is described previously in detail [16]. Chromosomal localization and order of markers were calculated using the MapMaker QTX program package (Whitehead Institute, MIT, Boston, MA, USA).

Micro-Computed Tomography

Morphologic properties were determined using micro-computed tomography (microCT) images. Specimens were scanned on a cone beam microCT scanner (GE Healthcare Biosciences). Each specimen was reconstructed with $18\mu\text{m} \times 18\mu\text{m} \times 18\mu\text{m}$ voxels to generate a 3D data image, which was further processed using GE Microview software. Standardized trabecular analysis volumes were created by selecting an analysis volume (Figure 1) with the following parameters: 15% of the specimen height in the axial direction and as large as possible in the anterior-posterior/medial-lateral plane, fit to the extreme ends of the trabecular cavity, in both the proximal and distal ends of each vertebra. This process involved user selection on 2-dimensional images in the x, y and z axis and interpolation using a spline function provided in the system software. From the analysis volumes, Bone Volume Fraction (V-BV/TV) and Trabecular Plate Number per Unit Length (V-Tb.N.) were calculated. Results from proximal and distal ends were averaged to create one BV/TV and one Tb.N. value for each vertebra.

In addition to the trabecular measures, whole bone geometric properties were calculated. Three analysis regions were selected: a distal region centered at 20.5% of the overall length from the distal end of the vertebra, a middle region centered at the mid-point of the bone, and a proximal region centered 20.5% of the overall length from the proximal end of the bone. Each of these regions encompassed the entire bone cross section and spanned 9% of the bone length (Figure 2). In the distal and proximal regions, which contain significant trabecular bone, the cross-sectional area was obtained using custom MATLAB and FORTRAN software. The distal and proximal cross-sectional areas are referred to as VCAD and VCAP, respectively, in the figures and tables. Cross sectional area was defined as the total area of bone tissue on each 2-dimensional slice of the microCT image, and included both trabecular and compact bone. In the middle region, which contains no trabecular bone, the following parameters were calculated using similar programs: cross sectional area (VCAM), VIML (I_{ML} , bending moment of inertia about a medial-lateral line through the center of gravity of the section), average shell thickness (VSHTH) at the anterior-lateral regions (Figure 2), and the standard deviation of the shell thickness (VSHSD) obtained every 10 degrees around the vertebral shell (a relative measure of the sharpness of vertebral protrusions). For each measurement, the calculations were conducted on each z slice that fit in the identified region, and then the results from all slices in that region were averaged. In addition, the overall height (length) of the vertebra (VHT, proximal-distal length) was determined.

Mechanical Testing

In order to achieve parallel loading surfaces, both endplates were machined using a pneumatic micro-endmill. An optimal balance between minimizing tissue removal and minimizing tipping of the bone during loading was achieved by removing 0.01" from each end of the vertebrae. All specimens were hydrated and at room temperature when machined. Mechanical properties were determined by loading the vertebrae to failure in compression. A servohydraulic testing machine (858 Mini Bionix II, MTS Systems, Minneapolis, MN) was used to test the bones to failure at a constant displacement rate of 0.5 mm/sec between parallel rigid loading platens. Load was measured on a 50-lb load cell (Model 41; Sensotec, Columbus, OH, USA) and platen-to-platen displacement was obtained using a linear variable differential transducer (010 MHR; Schaevitz Engineering, Pennsauken, NJ, USA) attached to the platens. Testing was conducted on hydrated specimens at room temperature. Load and displacement data were acquired and plotted for each specimen. Using a custom Matlab program, the following mechanical properties were determined for each vertebra: stiffness (VSTF), yield load (VYDL), displacement at yield load (VYDDS), ultimate load (VULLD), and displacement at ultimate load (VULDS). Specimens that broke during the milling procedure or immediately slipped/tipped upon loading were excluded from analysis. Approximately 509 specimens were included in the final mechanical data set.

Statistical Methods

A single-point, genome-wide search was performed for each trait to detect QTL that may be associated with the trait. To make the analysis consistent for all partially and fully informative markers, four-way informative markers were split into two sets of biallelic markers that were informative for either the maternally or paternally transmitted alleles. One-way ANOVA models, with trait as the dependent variable and biallelic marker as the factor with two levels, were used to perform genome-wide searches for all 185 biallelic markers. The strength of linkage associations between genetic markers and mechanical traits was evaluated using a permutation-based test of statistical significance. This test generates “experiment-wise” p-values. The phenotype and genotype data were permuted 1000 times to generate a null distribution for detection of QTL, and the resulting distribution compared to the actual, observed F statistic to provide the experimentwise adjusted p value. The use of the permutation testing follows directly from Churchill and Doerge (19) and also takes into account the multiple hypotheses (markers) that were tested in this search and avoid type I error inflation [19]. An experimentwise p 0.05 was the chosen criterion for inferring that a specific marker has a statistically significant linkage to a QTL of interest. The percent of variance in each mechanical trait that can be explained by genetic effects was estimated in a standard way from corresponding regression models. In addition to standard, single QTL analyses, computations were also performed after adjusting for mouse body weight measured at 3 and 18 months.

Results

Correlations among measures of vertebral size and shape

The availability of gene/trait association data for a wide range of distinct, but related, aspects of vertebral morphology provided an unprecedented opportunity to study the combined effects of morphogenesis and aging from a genetic perspective. The traits evaluated in the 18 month old mice show varying degrees of correlation among the 525 mice evaluated (509 for mechanical correlations) (Table 1). Results for adjusted analysis (weight at 3 and 18 months, data not shown) were consistent with those shown for unadjusted data. Several aspects of this correlation matrix are worth noting as a prelude to the genetic analysis: (a) V-BV/TV and V-Tb.N. are correlated more strongly to one another than either of them is to any of the other measures. (b) Vertebral height (VHT) is not strongly correlated to any of the other measures. (c) The other measures of vertebral shape and cross-sectional areas are correlated significantly to one another, with $0.23 < R < 0.87$, but not significantly associated with V-BV/TV or with VHT. A principal factors analysis (not shown) demonstrated that 78% of the variance could be partitioned into three principal factors, one with high loadings for VCAP, VCAM, VCAP, VIML, VSHTH, and VSHSD explaining 47% of the variance; one with high loadings for V-BV/TV and V-Tb.N. explaining 20% of the variance; and a third with high loadings only for VHT accounting for 12% of the variance. Note that many of these variables are expected to be highly correlated due to their mathematical interrelationships. For example, all else being equal, a greater shell thickness (VSHTH) will result in larger cross-sectional areas and VIML.

QTL that influence vertebral morphology and mechanical properties

Table 2 presents a summary of the QTL analysis of vertebral morphology and mechanical properties. Each line in the table represents a marker locus (maternal (M) or paternal (P)) that was found to be associated with the indicated trait with experimentwise $p < 0.05$, thus providing strong evidence that the chromosomal area near the marker contains at least one polymorphic locus (QTL) with an influence on the trait concerned. In many cases, the analysis revealed significant linkage to more than one of the markers on the same chromosome, an indication that more than one marker locus was sufficiently close to the QTL to distinguish among sets of mice with different alleles at the QTL in question. Where the QTL analysis showed that two or more marker loci on a given chromosome were significantly associated with a specific trait,

Table 2 presents only those markers for which the strength of association was strongest. In review of a complete listing of all markers found to have experimentwise $p < 0.05$ in this study (not shown), loci with significant effects on vertebral morphology are seen on maternal chromosomes 1, 2, 4, 5, and 17, and on paternal chromosomes 1, 2, 3, 4, 5, 7, 8, 9, 10, 11, 14 and 15. This set of 17 distinct polymorphisms represents a minimum estimate of the genetic complexity of the network of interactions affecting vertebral size and shape, because it is probable that at least some of the listed chromosomes may contain more than one locus that affects vertebral morphology. It is also likely that other chromosomes contain loci affecting C8 morphology that did not reach statistical significance in this study or are not polymorphic within this particular strain combination. Loci with significant effects on mechanical properties were found only on loci on maternal chromosomes 1, 9, and 17.

Multitrait plots for post-hoc analysis of genetic effects

The vertebral properties measured are likely to be related to one another in complex ways, because some factors - genetic or environmental - might alter several properties together, while others might be relatively specific for only one aspect of vertebral size, shape, or mechanical properties. To begin an exploration of these issues, we made use of a graphic approach. Figure 3 shows a collection of gene/trait association plots for the maternal alleles segregating in the UM-HET3 cross, and Figure 4 shows a similar set of plots for the segregating paternal alleles. In these “multitrait” plots, the horizontal axis corresponds to position of the genetic loci, with the telomeric (distal) end of each chromosome followed in the graphic by the centromeric (proximal) end of the succeeding chromosome, from chromosome 1 at the left through to the X chromosome at the right. Tick marks along the horizontal axis show the positions of the marker loci used during the genotyping process. Each of the 13 strips in the graphic represents a different phenotypic trait, as indicated at the left margin. Each bar in the plot indicates the strength of association between the trait in question and the marker locus segregating at that position from the maternal (Figure 3) or paternal (Figure 4) parent. The height of each bar corresponds to the negative of the logarithm (base 10) of the experimentwise p -value, so that a bar whose height is 3 corresponds to a p -value of 0.001. The horizontal line in each case corresponds to our significance criterion of experimentwise $p < 0.05$.

We can illustrate the potential usefulness of this graphical approach with several examples. Table 1 shows, for instance, a moderate degree of correlation ($R = 0.69$) between bone volume fraction V-BV/TV and trabecular plate number V-Tb.N., consistent with the idea that the factors that influence V-BV/TV and V-Tb.N. may overlap. Inspection of Figures 3 and 4 reveals several chromosomal regions (M5, P8, and P14, where M5 is an abbreviation for maternal chromosome 5) that influence both morphological properties. (The letter “A” is used in Figures 3 and 4 to draw attention to regions of interest in the comparison of QTL that modulate V-BV/TV and/or V-Tb.N.) It is possible that one or more of these chromosomes contains a QTL that influences both V-BV/TV and V-Tb.N.; alternately, each chromosome might contain two or more loci, one with effects on V-BV/TV and another that modulates V-Tb.N.. In contrast, the graphic also reveals several chromosomal regions that seem likely to have differential effects on these two traits. Chromosomes M1, M4, and P5, for example, have QTL with significant effects on V-BV/TV (using the experimentwise criterion as for Table 2). Inspection of the graphic shows that these regions do not contain segregating loci whose effects on V-Tb.N., in our experimental population, were strong enough to produce an experimentwise p -value < 0.05 (log score of 1.3). Such an observation suggests that these chromosomes may contain QTL that modulate V-BV/TV through a pathway that does not alter V-Tb.N.. Conversely, chromosome P1 contains at least one QTL with a significant effect on V-Tb.N., whose effect on V-BV/TV seems weak or absent.

A second example involves analysis of the genetic loci that influence the cross-sectional area of regions at the proximal end, middle, or distal end of the vertebral body (traits VCAP, VCAM, and VCAD in the figures). Chromosome M5 contains at least one QTL that influences the cross-section of the proximal and distal regions of the vertebra, but there is no evidence to suggest that this QTL influences the cross sectional area of the middle of the vertebra. QTL on P11 and P15 seem to have similar specificity for the ends of the vertebral body. Conversely, a QTL on M2 has a strong and significant effect on the VCAM trait, with no evidence for effects on VCAP or VCAD values. The QTL on P1 that influences VCAM may also be specific for the mid-section of the vertebra. Chromosomes M1 and M17 each contain QTL that influence all three indices of cross-sectional area, although it is not possible to judge if these effects represent single QTL that affect all three traits or multiple, closely spaced QTL on some of the chromosomes. Lastly, we note a region on P4 that has influence on the proximal end and middle of the vertebral body (VCAP and VCAM score), but seems less likely to exert a strong influence in the VCAD trait. The letter “B” is used in the two figures to designate the examples discussed in this paragraph.

The thickness of the vertebral shell (VSHTH) and the standard deviation of the thickness at multiple angles around the vertebral axis (VSHSD) are weakly, but significantly, correlated ($R = 0.38$, $p < 0.0001$) in our mouse population. Some chromosomal regions (P1 and M1) contain QTL influencing both traits. Other regions, in contrast, include QTL that seem to influence one trait but not the other: VSHTH appears to be specifically influenced by genes on P4, P5, P14, and M4, and VSHSD by a QTL on chromosome P9 (see areas indicated by letter “C” in the figures). Similarly, the height of the vertebra (VHT) is influenced by QTL on chromosomes P2 and P7 that do not appear to have effects on other aspects of vertebral morphology (letter “D” in Figure 4), as well as by QTL on P1, P14, and M1 that may also modulate other vertebral properties.

We detected three QTL that met experimentwise significance levels for mechanical properties. One QTL, which influenced ultimate load before failure, was mapped to a position near *D1Mit105*, 80 cM from the centromere of chromosome M1. Mice inheriting the C57BL/6J allele sustained higher loads before failure, consistent with the observation (Table 2) that the C57BL/6J allele at this marker was associated with greater V-BV/TV, and greater cross sectional area at top, midsection, and bottom of the vertebra, as well as greater shell thickness. A second QTL, located near *D17Mit46* on M17, also influenced ultimate load, consistent with the observation that the C57BL/6J allele at this marker locus was associated with significantly higher levels of cross-sectional area at each region of the vertebra. Potentially of greater interest was the QTL near *D9Mit12*, at 55 cM from the centromere of chromosome M9; mice inheriting the C57BL/6J allele at this locus had significantly higher displacement seen at ultimate load. We note (Figure 3 and Table 2) that none of the chromosome 9 marker loci had significant effects on any of the measured morphological properties of the vertebra, consistent with the idea that the locus detected on M9 might influence the mechanical properties of the vertebra independent of any alteration in its size or shape, perhaps through an effect on the material properties of the bone tissue.

Co-ordinate and separate genetic influence on vertebral and femoral traits

Virtually all of the mice used for the QTL analysis of vertebral morphology were also evaluated for a series of femoral traits; QTL maps for various measures of femoral size and shape have been reported previously [16,17,20-24]. Four of these traits are included for comparison at the bottom of Figures 3 and 4. FCSA refers to the cross sectional area of the femur at a mid-diaphyseal section. FCTH is a measure of the thickness of the cortex of the femur. FSF, the “shape factor,” is calculated as the ratio of the minimum outer fiber length to the maximum outer fiber length as previously described [16]; an FSF of 1.0 would correspond to a perfectly

round cross section, and smaller values refer to more elliptical cross sections. These traits were abbreviated as CSA, CortTh, and SF in the original publication, but are here abbreviated differently to facilitate comparison with the vertebral traits. FLEN is the length of the femur.

The graphics permit comparison of genetic influences on vertebral and femoral properties. We have already noted, for example, the presence on both M1 and P1 of loci that modulate various aspects of vertebral morphology. It is thus noteworthy that both M1 and P1 also contain QTL that influence the shape of the femoral cross section (FSF); P14, also, contains QTL with influences on FSF as well as QTL that modulate vertebral size and shape. Other QTL with effects on FSF, in contrast, are on chromosomes (M11 and M12) without any detectable impact on vertebral properties.

The combined data set allows us to ask if genes that modulate the cross-sectional area of the femur also affect vertebral properties. All four of the significant QTL for FCSA are on chromosomes (P3, P4, P8, and P15) that influence vertebral traits, too, but in different ways depending on the locus involved. Thus P3 has QTL that influence VIML and perhaps VCAP; P4 bears QTL with effects on VIML, VSHTH, VCAP, and VCAM, as well as femur cortical thickness FCTH; P8 includes QTL for VIML, V-Tb.N., and V-BV/TV; and P15 genes affect only VCAP and VCAD.

The length of the femur is influenced, in this cross, by QTL on 5 chromosomes: M5, M9, M13, M17, and P2. Two of these - those on M9 and M13 - do not seem to have detectable influence on any of the tested vertebral properties. P2 has QTL that influence both FLEN and VHT, although we cannot tell without higher resolution maps if these two traits are influenced by the same QTL; the DBA/2J allele on chromosome P2 is associated with higher levels of both FLEN and VHT. The other two chromosomes, M5 and M17, both exert an influence on VCAP and VCAD; the latter also has QTL with effects on VCAM. The BALB/cJ allele on M5 is associated with higher levels of VCAD, VCAP, and FLEN; similarly, it is the C57BL/6J allele on M17 that is associated with higher levels of FLEN, VCAP, VCAM, and VCAD. These complex patterns show that the final size and shape of the vertebrae must be influenced by a multitude of polymorphic loci, some of which may also modulate femoral traits, and others of which do not.

SNP-based higher resolution map of chromosome 1

The initial set of QTL maps, presented in Figures 3 and 4, depended on a set of SSLP (simple sequence length polymorphism) markers, spaced at distances of approximately 15 cM across the genome. We have begun to develop a set of SNP (single nucleotide polymorphism)-based markers to provide more precise estimates of QTL positions within each chromosome. Figure 5 presents an illustration of the usefulness of this system for dissection of the chromosome 1 loci that affect bone morphology in the UM-HET3 system. The first panel shows results using 16 SNPs distributed across chromosome M1 and the second panel displays data from 21 SNPs on P1. Each panel shows point-wise p-values plotted against position on the maternal and paternal Chromosome 1 for five traits, four of which achieved experiment-wise significance in the genome scan and one of which (V-Tb.N. for maternal genes; V-BV/TV for paternal genes) did not. The vertical axis shows the strength of the gene/trait relationship, as the negative logarithm of the p-value calculated from the t-test contrasting mice of the two genotypic classes. A high score - for example, the score of 13.7 for VIML at position 161 on M1 - reflects a large genetic effect, in this case differences between mice inheriting the C57BL/6J allele and the BALB/cJ allele for which $p(t) = 10^{-13.7}$. Lower scores reflect proportionally smaller differences between groups of mice differing at the SNP position indicated on the horizontal axis. The graphic suggests strongly that the M1 QTL that influences FSF is located more proximally than the strongest of the QTL that modulate V-BV/TV, VHT, and VIML, although the data do not exclude the idea that M1 may have two QTL for the vertebral properties, one near 160

million base pairs (mpb) and another between 100-140 mpb. The second plot suggests a paternal allele for FSF between 80-100 mpb, and is consistent with hypotheses of at least two QTL for V-TB.N. and VHT, one distal (~160 mpb) and the other more proximal (90-140 mpb).

Discussion

The UM-HET3 system brings several advantages to QTL searches. First, and most importantly, the founder strains were chosen based on genetic variation among inbred strains, rather than phenotype variation. At first, this may seem counter-intuitive, and is not an advantage for any single phenotype. The advantage is that many investigators can use the same population of animals, regardless of the phenotypes in which they are interested. The founders were not chosen to be a “high” and a “low” for a single phenotype. Consequently, we can use one large population for studying hundreds of phenotypes, in dozens of organs and tissues. This is extremely important when studying late-life phenotypes, since the housing cost for mice are very high and this allows the costs of one population to be shared by many investigators. Second, since many phenotypes are measured on each animal, the large database of phenotypes can be compared between phenotypes, identifying novel or unexpected connections between phenotypes within a single individual. Third, the four-way cross gives a population with greater genetic variation than a F2 intercross. At any single locus, the population has four possible genetic pairings (all four possible pair-wise heterozygous combinations, in a population ratio of 1:1:1:1), rather than three (the two homozygotes and the single heterozygote, 1:2:1). Fourth, the large number of possible segregating polymorphic loci can lead to novel geneXgene interactions. These can be detected, even in complex interactions as illustrated in our recent work examining IGF-1 (28). The UM-HET3 population is not intended to supplant studies using F2 intercrosses, but only to provide a rigorous, reproducible, alternative breeding structure.

The QTL data in Table 2 imply that at least 13 mouse chromosomes contain loci that influence the size, shape, and/or mechanical properties of the C8 vertebra. This is almost certainly an underestimate, for several reasons. (1) We cannot, without further data, tell whether a specific association between a marker locus and a trait of interest represents one, two, or more linked QTL with an effect on the trait. (2) The mapping strategy will detect only those loci that are polymorphic either between BALB/c and C57BL/6, or between C3H/HeJ and DBA/2. Other inbred mouse stocks, and wild mice more generally, almost certainly contain polymorphisms that influence vertebral development but which do not discriminate within the inbred grandparents used to produce UM-HET3 mice. (3) The mapping procedure has a sizable false negative rate. It is likely that many loci, polymorphic in our segregating cross, influence vertebral size, shape, and/or mechanical properties, but did not produce an effect large enough in our sample to reach our conservative criteria for experimentwise significance. Figures 3 and 4, for example, show many examples of gene/trait associations whose strength is suggestive of a linked QTL, but which did not achieve significance in our study. (4) In several cases we find evidence for QTL with effects of a given trait segregating from both the maternal and paternal side. VCAM, for example, can be modulated by QTL linked to maternal or paternal *DIMit105* at 80 cM on chromosome 1. It is not possible from the current data set to know if the maternal and paternal QTL are located at the same genetic locus, or merely at loci that are by coincidence near to one another. In some cases, though, it seems most likely that the maternal and paternal chromosomes bear different QTL.

It is also possible that some of the QTL listed in Table 2 represent false positives. Although the significance criterion chosen reduces Type I error that might be expected from simultaneous analysis of multiple marker loci, it does not adjust for the number of traits evaluated in the study overall. For each individual QTL in Table 2, we can be at least 95% confident that the

association does not reflect chance alone, but we cannot have a similar degree of confidence that the set of linkages shown in the table is free of false positive findings.

The traits we have analyzed are, not surprisingly, correlated to various degrees, and many of the correlations reach a convincing level of statistical confidence (see Table 1). The correlations among traits represent a mixture of genetic effects (i.e. genetic alleles that influence both traits) and non-genetic effects, and within the genetic realm some may have a direct influence (for example, by regulating the level of a bone cell protein) and others have only indirect influence (for example, by regulating appetite, activity level, weight, hormone responses, etc.) The graphical depictions used in Figures 3 and 4 provide some initial insight into these complexities. It is clear, for example, that some polymorphisms, such as the P5 QTL that affects V-BV/TV, are able to exert their effect without a detectable influence on V-TB.N., while others, such as the QTL on P1, modulate V-TB.N. without an apparent effect on V-BV/TV. In contrast, some chromosomes (such as P14) contain QTL that influence V-TB.N. and QTL that influence V-BV/TV. In this case the C3H/HeJ allele is associated both with higher V-BV/TV and higher V-TB.N.. This co-localization suggests the hypothesis that a single QTL on P14 may influence both aspects of vertebral morphology. These findings may also suggest differences in structure function relationships between the skeletons of mice and humans. For example, in humans high correlations have been reported between BV/TV and TB.N (25,26). An explanation for this correlation has been the observation that trabecular thickness has a low variation in human metaphyseal regions. As a result, it might be expected to find QTL that influence both BV/TV and TB.N. In the current mouse data, the modest correlation between BV/TV and TB.N in association with QTL that influence TB.N and BV/TV together and independently suggest that trabecular thickness may vary more and be a more important factor in structure function relationships. It might also reflect a scaling issue related to the small number of trabeculae in individual bones and the subsequent important mechanical role each trabecular strut may play.

Similar hypotheses can be drawn by comparison of the maps for vertebral properties with maps of QTL that influence femoral size and shape. For example, of the five QTL that influence FLEN (using experiment-wise $p < 0.05$), only one maps to a chromosome (P2) containing a QTL for VHT; the others (on M5, M9, M13, and M17) appear not to affect VHT to a detectable extent. It is the DBA/2J allele on P2 that is associated with higher levels of both FLEN and VHT. Conversely, QTL for VHT on chromosomes M1, P1, P7, and P14 do not appear to affect the length of the femur. It is apparent that much of the genetic influence on the length of the vertebra is mediated by loci that do not influence femur length, and also that P2 might well contain a locus with influence on both the axial and peripheral skeleton. These contrasts may be very instructive in future work on increasing the fidelity of the search for specific genes that regulate the development or adaptation of the skeleton. Overlapping regions (between axial and peripheral sites) may suggest regulation at the level of bone growth as influenced by systemic factors mediating a somewhat symmetric pattern of growth. Alternatively, they may regulate basic morphologic scale features of bone ECM structure. On the other hand, the non-overlapping regions might signify local regulators of morphology as influenced by site specific mechanical or biologic conditions.

There are many other examples in Figures 3 and 4 of chromosomal segments that do, or do not, influence vertebral properties in a coordinated fashion. Some of these have been pointed out explicitly in the Results section, and others of equal interest can be inferred from the two figures. Our current data set is designed to permit exploratory comparisons of QTL maps for multiple traits. This set of UM-HET3 mice, for example, has been evaluated for body weight at multiple ages [20]; levels of leptin, corticosterone, and thyroxine as well as IGF-I at varying ages [21]; multiple measures of immune status [22,23]; tests of age-sensitive cellular and biophysical properties [24]; and multiple tests of the geometric and mechanical properties of the femur [16,17]. Comparative analysis to look for QTL that influence any of these properties

either along with, or independently of, other traits of interest may be facilitated by the comparative mapping process illustrated in Figures 3 and 4.

Another group has conducted a genome-wide survey for vertebral properties in mice [18]. Mice were bred as the F2 progeny of (C57BL/6J x C3H/HeJ)F1 mice, and evaluated at 4 months of age. This breeding strategy, unlike the four-way cross method, considers only two possible alleles at each locus, but produces some progeny that are homozygous for each of the two grandparental alleles, and thus allows detection of dominant and recessive alleles. It is difficult to compare the results of this study with our own data, not only because of differences in the age of the mice, specific traits measured, and genetic strategy, but also because our breeding plan does not permit a direct comparison between the effects of C57BL/6J and C3H/HeJ alleles. Nonetheless, it is of interest to note that both our study and the previous report documented significant effects of QTL on chromosomes 1, 4, 8, and 14 on bone volume fraction (BV/TV ratio in 18). In contrast, QTL on chromosomes 9, 12, 13, and 17 documented in the F2 cross do not seem to modulate V-BV/TV in our own population. Conversely, our population provided evidence for one or more QTL for V-BV/TV on both M5 and P5, a chromosome that did not significantly affect BV/TV ratio in the F2 cross; it is possible that these chromosome 5 QTL influence V-BV/TV only at later ages. A similar partial overlap applies to the emerging QTL maps for V-TB.N. (18): both studies find QTL on chromosomes 1 and 8, but the published report noted QTL on chromosomes 9, 10, 12, and 13 which do not have any apparent effect in our cross. Conversely, the V-TB.N. QTL we see on M5 is not detected in the F2 model.

The results of this study demonstrated a large number of loci associated with morphologic features of the vertebrae while only a few loci were related to mechanical properties. There may be two reasons that explain this finding. First, the mechanical properties of the vertebrae are dependent on a number of shape and geometric factors as well as the inherent properties of the tissue ECM. While the material properties of the ECM can be considered an independent factor, a few geometric measures likely have a dominant effect on the mechanical behavior, namely a cross sectional area measure and the thickness of the cortical walls. Secondly, the mechanical tests on these bones are difficult to apply and the variability due to testing conditions may be large in comparison to the variations due to morphologic and material properties.

This study evaluated female mice in an effort to increase statistical power to detect QTL, since it excludes one parameter (gender) known to have a major effect on physiology. It must be noted, however, that there are important limitations to the use of 18 month-old female mice in this QTL study. As implied earlier, the measured phenotypic properties probably reflect a combination of effects from growth, maturation, and adaptation to environmental stimuli over the life of the animals. As a result, some of the relationships between genotype and phenotype will be blurred since they may be influenced by physiologic factors other than age. The QTL from this study must therefore be considered a starting point for continuing studies targeted at separating the effects of loci that may contribute to age related alterations or adaptation of skeletal properties as a result of responses to stimuli occurring during aging from those that prescribe properties during growth and development that result in the observed variations in the older skeleton. The findings are also difficult to compare to others in the literature, since most prior studies utilized animals less than 6 months of age. In fact, it is possible that some of the differences in loci between this study and others may represent the first separation of QTL associated with age-related adaptation from those reflecting development and maturation.

While insight has been gained from studying murine vertebrae, several observations during the course of this work raise issues regarding the correspondence of mouse data to properties in humans. The architecture and shape of murine vertebrae are considerably different from human vertebrae. While human vertebrae are primarily composed of trabecular bone with a

thin shell of dense trabecular bone [25], murine vertebrae have a proportionally much thicker shell. In addition, the central portion of murine vertebrae does not generally contain trabecular struts. The small size of the vertebrae makes it very difficult to conduct mechanical tests. In order to test in compression, endplates must be machined or the ends must be potted in order to provide consistent loading surfaces. Thus, it may be beneficial to look at other, larger animals for future study or examine other murine anatomic sites relatively rich in trabecular bone, such as the femoral head or proximal tibia.

Acknowledgments

This study was supported by the National Institutes of Health P30-AG08808, R01 AG-11687-11 and P30 AR-46024. The authors thank Gretchen Buehner, Cari R. Bryant, Richard Eikstadt, Adrienne L. Prysock, Jessica Sewald, Margaret Vergara, Stephen Roller, Jaclynn Kreider, Leonard Lee, and Suzanne K. Volkman for their contributions to this study.

References

- [1]. U.S. Department of Health and Human Services. Bone Health and Osteoporosis. A Report of the Surgeon General. U.S. Department of Health and Human Services, Office of the Surgeon General; Rockville, MD: 2004.
- [2]. Hallberg I, Rosenqvist AM, Kartous L, Lofman O, Wahlstrom O, Toss G. Health-related quality of life after osteoporotic fractures. *Osteoporos Int* 2004;15:834–41. [PubMed: 15045468]
- [3]. Ciarelli TE, Fyhrie DP, Schaffler MB, Goldstein SA. Variations in three-dimensional cancellous bone architecture of the proximal femur in female hip fractures and in controls. *J Bone Miner Res* 2000;15:32–40. [PubMed: 10646112]
- [4]. Langman CB. Genetic regulation of bone mass: from bone density to bone strength. *Pediatr Nephrol* 2005;20:352–5. [PubMed: 15633054]
- [5]. Huang QY, Xu FH, Shen H, Zhao LJ, Deng HY, Liu YJ, Dvomyk V, Conway T, Davies KM, Li JL, Liu YZ, Recker RR, Deng HW. A second-stage genome scan for QTLs influencing BMD variation. *Calcif Tissue Int* 2004;75(2):138–43. [PubMed: 15085314]
- [6]. Karasik D, Cupples LA, Hannan MT, Kiel DP. Age, gender, and body mass effects on quantitative trait loci for bone mineral density: the Framingham Study. *Bone* 2003;33:308–16. [PubMed: 13678771]
- [7]. Koller DL, Schriefer J, Sun Q, Shultz KL, Donahue LR, Rosen CJ, Foroud T, Beamer WG, Turner CH. Genetic effects for femoral biomechanics, structure, and density in C57BL/6J and C3H/HeJ inbred mouse strains. *J Bone Miner Res* 2003;18:1758–65. [PubMed: 14584885]
- [8]. Peacock M, Koller DL, Fishburn T, Krishnan S, Lai D, Hui S, Johnston CC, Foroud T, Econs MJ. Sex-specific and non-sex-specific quantitative trait loci contribute to normal variation in bone mineral density in men. *J Clin Endocrinol Metab* 2005;90:3060–6. [PubMed: 15741260]
- [9]. Turner CH, Sun Q, Schriefer J, Pitner N, Price R, Bouxsein ML, Rosen CJ, Donahue LR, Shultz KL, Beamer WG. Congenic mice reveal sex-specific genetic regulation of femoral structure and strength. *Calcif Tissue Int* 2003;73:297–303. [PubMed: 14667144]
- [10]. Kammerer CM, Schneider JL, Cole SA, Hixson JE, Samollow PB, O'Connell JR, Perez R, Dyer TD, Almasy L, Blangero J, Bauer RL, Mitchell BD. Quantitative trait loci on chromosomes 2p, 4p, and 13q influence bone mineral density of the forearm and hip in Mexican Americans. *J Bone Miner Res* 2003;18:2245–52. [PubMed: 14672361]
- [11]. Ralston SH, Galwey N, MacKay I, Albagha OM, Cardon L, Compston JE, Cooper C, Duncan E, Keen R, Langdahl B, McLellan A, O'Riordan J, Pols HA, Reid DM, Uitterlinden AG, Wass J, Bennett ST. Loci for regulation of bone mineral density in men and women identified by genome wide linkage scan: the FAMOS study. *Hum Mol Genet* 2005;14:943–51. [PubMed: 15746152]
- [12]. Benes H, Weinstein RS, Zheng W, Thaden JJ, Jilka RL, Manolagas SC, Shmookler Reis RJ. Chromosomal mapping of osteopenia-associated quantitative trait loci using closely related mouse strains. *J Bone Miner Res* 2000;15:626–33. [PubMed: 10780854]
- [13]. McCreadie BR, Goldstein SA. Biomechanics of fracture: is bone mineral density sufficient to assess risk? *J Bone Miner Res* 2000;15:2305–2308. [PubMed: 11127195]

- [14]. Schnitzler CM. Bone quality: a determinant for certain risk factors for bone fragility. *Calcif Tissue Int* 1993;53:S27–S31. [PubMed: 8275376]
- [15]. Burr DB. Bone quality: understanding what matters. *J Musculoskel Neuron Interact* 2004;4:184–186.
- [16]. Volkman SK, Galecki AT, Burke DT, Paczas MR, Moalli MR, Miller RA, Goldstein SA. Quantitative trait loci for femoral size and shape in a genetically heterogeneous mouse population. *J Bone Miner Res* 2003;18:1497–1505. [PubMed: 12929939]
- [17]. Volkman SK, Galecki AT, Burke DT, Miller RA, Goldstein SA. Quantitative trait loci that modulate femoral mechanical properties in a genetically heterogeneous mouse population. *J Bone Miner Res* 2004;19:1497–505. [PubMed: 15312250]
- [18]. Bouxsein ML, Uchiyama T, Rosen CJ, Shultz KL, Donahue LR, Turner CH, Sen S, Churchill GA, Muller R, Beamer WG. Mapping quantitative trait loci for vertebral trabecular bone volume fraction and microarchitecture in mice. *J Bone Miner Res* 2004;19:587–599. [PubMed: 15005846]
- [19]. Churchill GA, Doerge RW. Empirical threshold values for quantitative trait mapping. *Genetics* 1994;138:963–971. [PubMed: 7851788]
- [20]. Miller RA, Harper JM, Galecki A, Burke DT. Big mice die young: early life body weight predicts longevity in genetically heterogeneous mice. *Aging Cell* 2002;1:22–9. [PubMed: 12882350]
- [21]. Harper JM, Galecki AT, Burke DT, Pinkosky SL, Miller RA. Quantitative trait loci for insulin-like growth factor I, leptin, thyroxine, and corticosterone in genetically heterogeneous mice. *Physiol Genomics* 2003;15:44–51. [PubMed: 12865502]
- [22]. Jackson AU, Fornes A, Galecki A, Miller RA, Burke DT. Multiple-trait quantitative trait loci analysis using a large mouse sibship. *Genetics* 1999;151:785–95. [PubMed: 9927469]
- [23]. Jackson AU, Galecki AT, Burke DT, Miller RA. Genetic polymorphisms in mouse genes regulating age-sensitive and age-stable T cell subsets. *Genes Immun* 2003;4:30–9. [PubMed: 12595899]
- [24]. Wisser KC, Schauerte JA, Burke DT, Galecki A, Chen S, Miller RA, Gafni A. Mapping tissue-specific genes correlated with age-dependent changes in protein stability and function. *Arch Biochem Biophys* 2004;432:58–70. [PubMed: 15519297]
- [25]. Mosekilde L. Age-related changes in bone mass, structure, and strength - effects of loading. *Z Rheumatol* 2000;59:1–9. [PubMed: 10769428]
- [26]. Goulet RW, Goldstein SA, Ciarelli MJ, Kuhn JL, Brown MB, Feldkamp LA. The Relationship Between the Structural and Orthogonal Compressive Properties of Trabecular Bone. *Journal of Biomechanics* 1994;27:375–389. [PubMed: 8188719]
- [27]. Goldstein SA, Goulet R, McCubbrey D. Measurement and Significance of Three Dimensional Architecture to the Mechanical Integrity of Trabecular Bone. *Calcified Tissue International* 1993;53:S127–S133. [PubMed: 8275366]
- [28]. Hanlon P, Lorenz A, Shao Z, Harper J, Galecki AT, Miller RA, Burke DT. Three-locus and four-locus QTL interactions influence mouse insulin-like growth factor-I. *Physiological Genomics* 2006;26:46–54. [PubMed: 16782841]

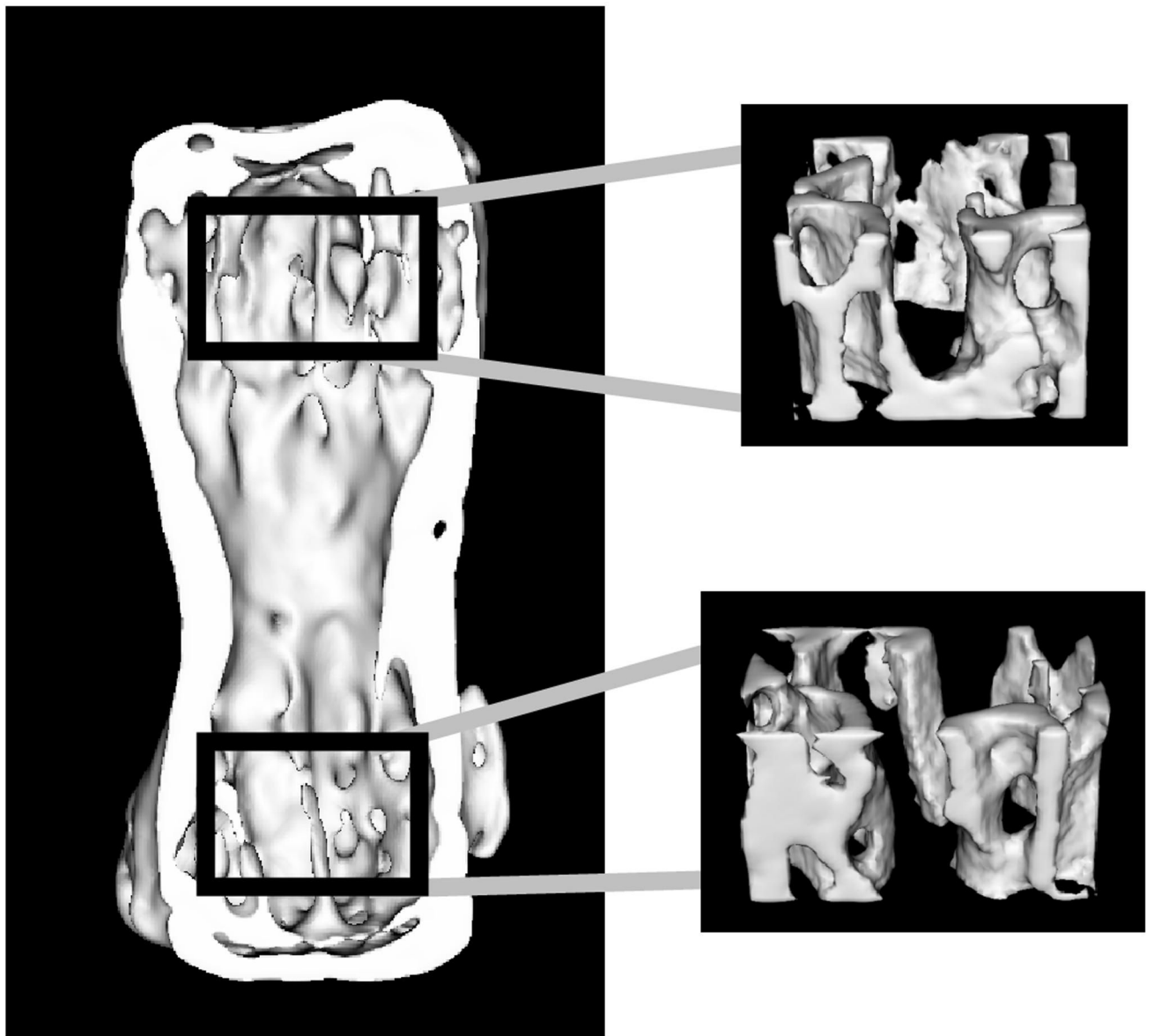


Figure 1.

Location of analysis regions for trabecular bone architecture.

Proximal and distal trabecular bone regions were obtained by fitting a box 15% of the specimen height in the axial direction and as large as possible in the anterior-posterior/medial-lateral plane, in the extreme ends of the trabecular cavity. Analyses of V-TB.N. and V-BV/TV were conducted separately for each region, then averaged to obtain one value for each specimen.

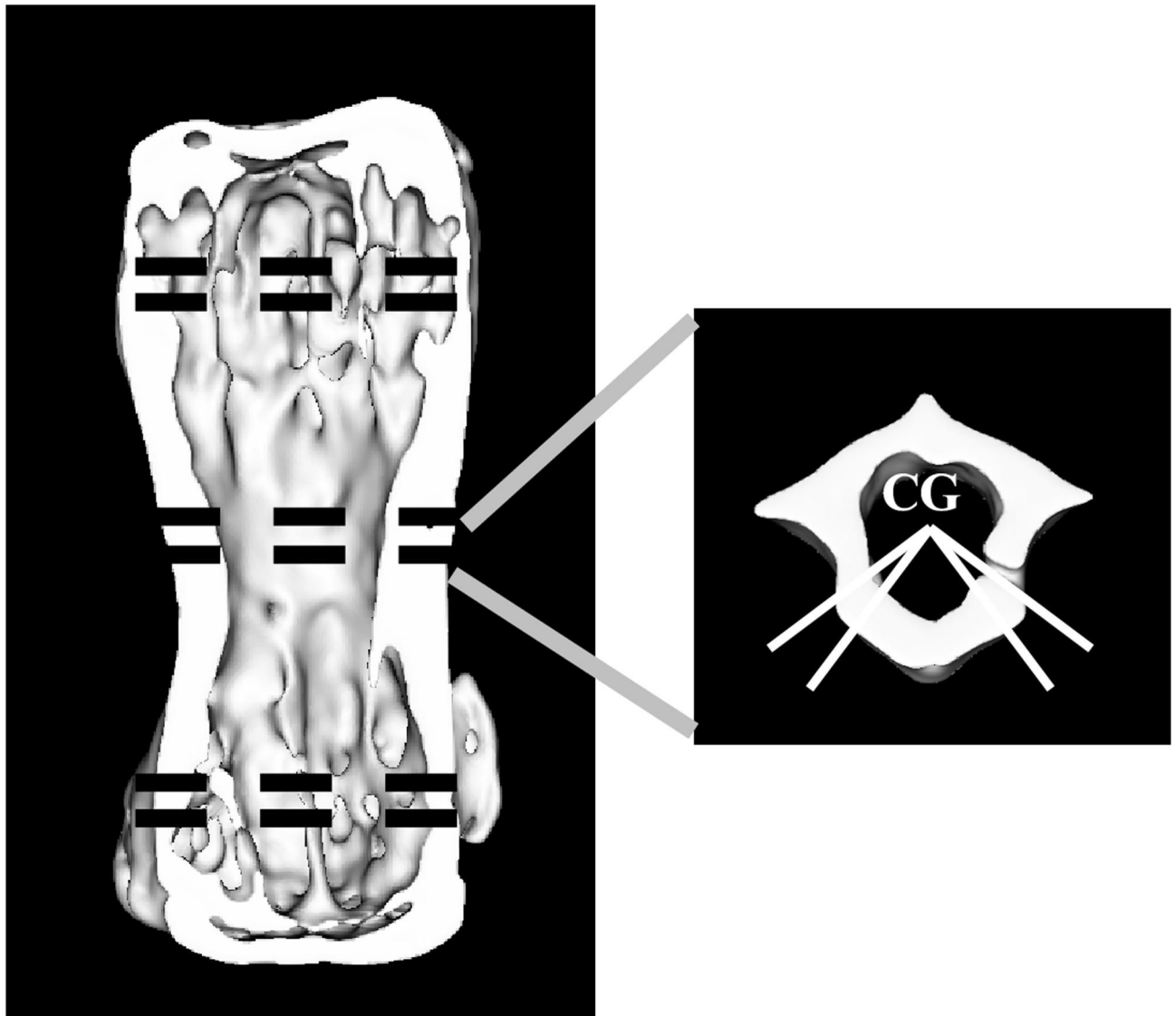


Figure 2.

Location of analysis regions for whole-bone geometric parameters.

Shell thickness (VSHTH) was calculated from the average thickness of the shell along four lines originating at the center of gravity (CG) of the central section, each 40 or 50 degrees anterior to a medial-lateral line drawn through the center of gravity of the section. Other measurements are described in the text.

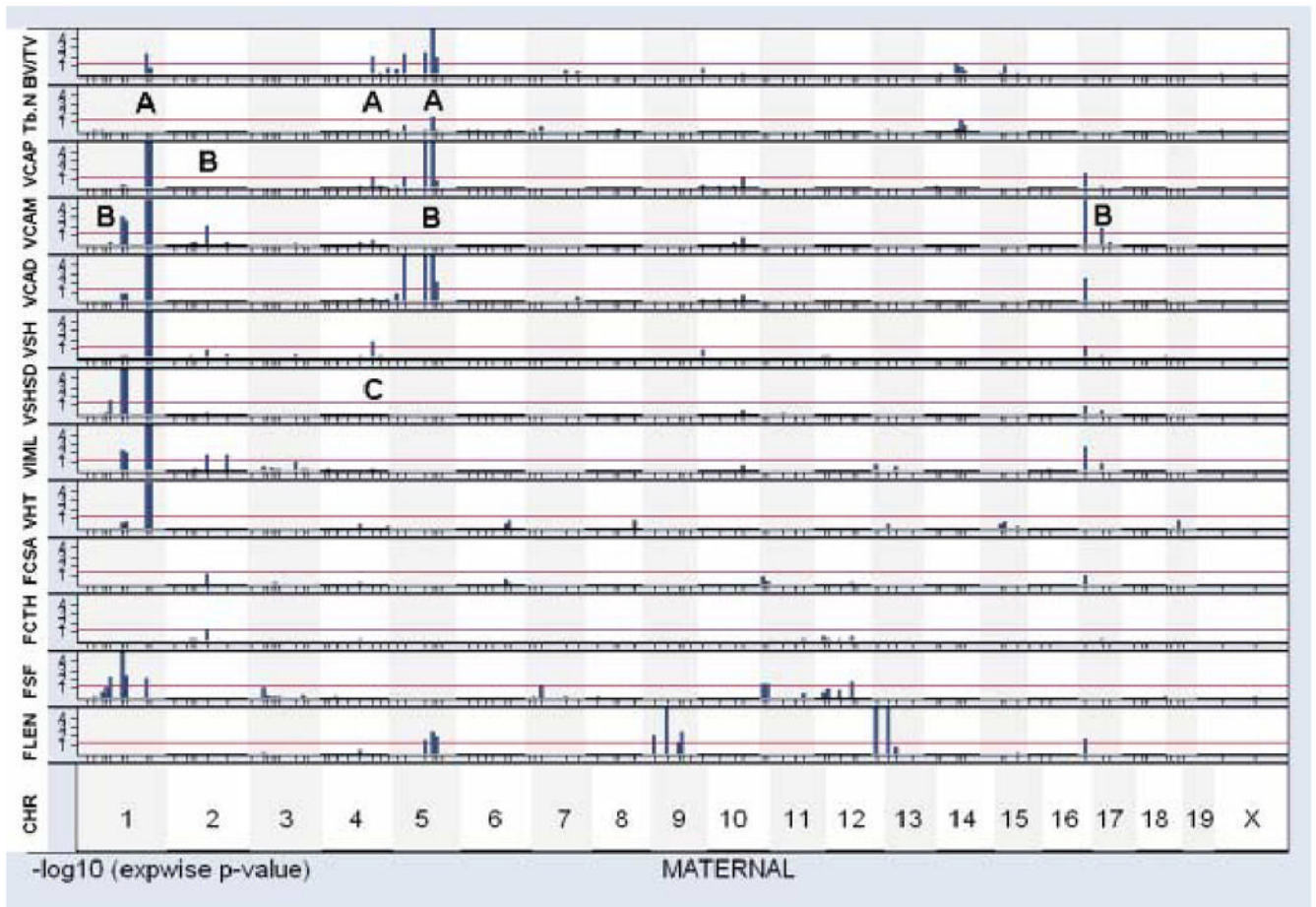


Figure 3.

Graphical display of maternal QTL for selected traits.

Each strip displays gene/trait associations across the genome, with chromosome 1 at the left and the X chromosome at the right. Marker loci are shown as tick marks below each plot, with centromeric markers at left and telomeric markers at right. The vertical axis shows a measure of gene/trait association, in this case the negative logarithm of the experimentwise p-value, truncated at 4 (corresponding to $p < 0.0001$). The horizontal red line shows those loci that reach our chosen significance criterion, i.e. experimentwise $p < 0.05$. The light shading (vertical strips, top to bottom of the page) indicates boundaries of each chromosome. Traits shown, top to bottom, are bone volume fraction (V-BV/TV); trabecular plate number (V-TB.N.), vertebral cross sectional area for the proximal end (VCAP), vertebral cross sectional area for middle (VCAM), vertebral cross sectional area for distal end (VCAD), vertebral shell thickness (VSHTH), standard deviation of vertebral shell thickness (VSHSD), moment of inertia about a medial-lateral line (VIML), vertebral height (VHT), femur cross sectional area (FCSA), femur cortical thickness (FCTH), femur shape factor (FSF), and femur length (FLEN).

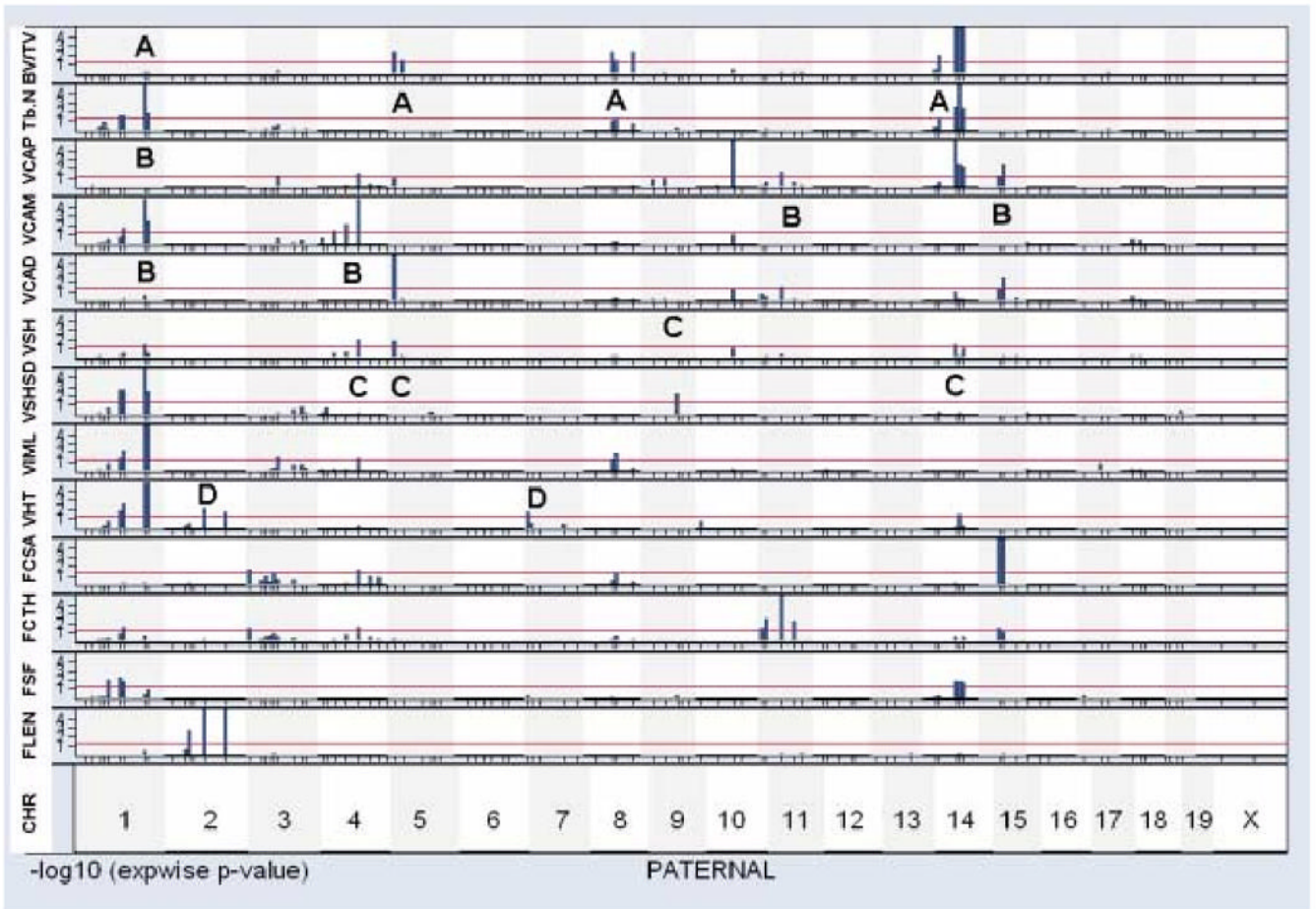


Figure 4.
 Graphical display of paternal QTL for selected traits.
 Data are presented in the same manner as Figure 3.

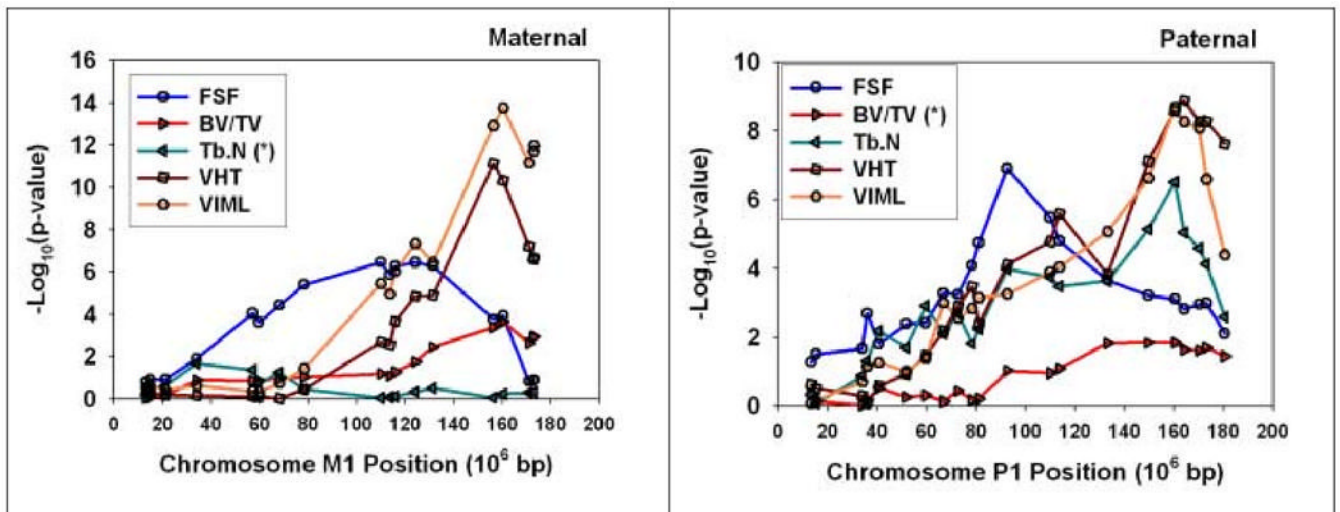


Figure 5.

Fine structure QTL maps for selected traits on maternal (first) and paternal (second) chromosome 1 of the UM-HET3 cross. The vertical axis shows an estimate of the difference between mice of different genotype classes, measured as the negative logarithm of the probability of the Student's t-test statistic. Each point represents an estimate of this value for mice distinguished by different SNP genotypes at the position shown on the horizontal axis. Five traits are shown on each plot; the (*) sign indicates in each case the trait for which there was no statistically significant QTL on the chromosome indicated.

TABLE 1

Correlations Among Vertebral Morphologic Traits in UM-HET3 Mice at 18 Months of Age Pairwise Pearson correlation coefficients (R) for each pair of indicated vertebral morphological measures. N ~ 525 for each pair of traits. Without adjustments for multiple comparisons, R = 0.12 corresponds approximately to p = 0.01, and R = 0.14 corresponds to p = 0.001. Using Bonferroni corrections, R = 0.13 corresponds to p = 0.05, and R ≥ 0.2 (shown in boldface) corresponds to p < 0.0001.

	V-BV/IV	V-TB,N	VCAP	VCAM	VCAD	VIML	VSHTH	VSHSD
V-TB,N	0.69							
VCAP	0.56	0.17						
VCAM	0.20	-0.08	0.65					
VCAD	0.42	0.05	0.84	0.71				
VIML	0.13	-0.08	0.54	0.87	0.61			
VSHTH	0.21	-0.06	0.59	0.81	0.67	0.62		
VSHSD	0.08	-0.03	0.23	0.63	0.32	0.55	0.38	
VHT	0.05	-0.04	0.11	0.12	0.03	0.15	0.00	-0.03

QTL Influencing Vertebral Traits in 18 Month Old UM-HET3 Mice Position in cM and bp is measured from centromeric end. Experiment-wise p-values and percent effect of each QTL on the given trait are presented. (M) and (P) designate maternal and paternal loci, respectively. The final column shows which of the maternal or paternal grand-parental strains contributed genes associated with greater and lesser values for the trait. C= BALB/c; B6= C57BL/6J; C3= C3H/HeJ; D= DBA/2J.

Table 2

Trait	Locus	position (cM)	position (10 ⁶ bp)	p-exp	% effect	comparison
Bone Volume Fraction (V-BV/TV TV)	D1Mit105(M)	80	161.63	0.004	3.99	C<B6
	D4Mit170(M)	67	136.22	0.009	3.62	C>B6
	D5Mit251(P)	12	25.44	0.004	4.36	C3<D
	D5Mit25(M)	61	111.79	0.001	7.07	C>B6
	D8Mit42(P)	71	126.57	0.004	3.92	C3<D
Trabecular Plate Number (V-TB.N.)	D14Mit170(P)	63	97.46	0.001	8.40	C3>D
	D1Mit105(P)	80	161.63	0.001	6.06	C3<D
	D5Mit25(M)	61	111.79	0.029	3.08	C>B6
	D8Mit51(P)	41	88.13	0.042	2.92	C3<D
	D14Mit170(P)	63	97.46	0.001	5.98	C3>D
Cross sectional area, distal (VCAD)	D1Mit105(M)	80	161.63	0.001	7.17	C<B6
	D5Mit251(P)	12	25.44	0.001	5.65	C3<D
	D5Mit205(M)	45	92.81	0.001	7.44	C>B6
	D11Mit156(P)	34	63.96	0.028	2.93	C3>D
	D15Mit63(P)	29	65.69	0.003	4.25	C3>D
Cross sectional area, middle (VCAM)	D17Mit46(M)	10	24.56	0.003	3.98	C<B6
	D1Mit105(M)	80	161.63	0.001	13.04	C<B6
	D1Mit105(P)	80	161.63	0.001	7.02	C3>D
	D2Mit58(M)	51	109.20	0.007	3.73	C<B6
	D4Mit155(P)	50	100.28	0.001	5.66	C3>D
Cross sectional area, proximal (VCAP)	D17Mit46(M)	10	24.56	0.001	5.62	C<B6
	D1Mit105(M)	80	161.63	0.001	8.23	C<B6
	D4Mit155(P)	50	100.28	0.034	3.13	C3>D
	D5Mit25(M)	61	111.79	0.001	6.05	C>B6
	D10Mit230(P)	49	90.39	0.001	4.83	C3>D
Shell thickness (VSHTH)	D11Mit156(P)	34	63.96	0.020	3.18	C3>D
	D14Mit263(P)	44	80.10	0.001	4.95	C3>D
	D15Mit63(P)	29	65.69	0.003	3.98	C3>D
	D17Mit46(M)	10	24.56	0.024	3.17	C<B6
	D1Mit206(M)	96	174.31	0.001	5.69	C<B6
Shell thickness standard deviation (VSHSD)	D1Mit105(P)	80	161.63	0.045	3.03	C3>D
	D4Mit155(P)	50	100.28	0.013	3.59	C3>D
	D4Mit170(M)	67	136.22	0.014	3.65	C>B6
	D5Mit251(P)	12	25.44	0.014	4.18	C3<D
	D14Mit263(P)	44	80.10	0.046	2.93	C3>D
Moment of inertia (VIML)	D1Mit105(M)	80	161.63	0.001	10.57	C<B6
	D1Mit105(P)	80	161.63	0.001	7.64	C3>D
	D9Mit110(P)	48	91.85	0.005	4.03	C3>D
	D1Mit105(M)	80	161.63	0.001	11.72	C<B6
	D1Mit105(P)	80	161.63	0.001	8.28	C3>D
Vertebral Height (VHT)	D2Mit285(M)	86	153.66	0.017	3.51	C<B6
	D3Mit73(P)	40	115.17	0.034	3.07	C3<D
	D4Mit155(P)	50	100.28	0.036	3.01	C3>D
	D8Mit51(P)	41	88.13	0.011	3.48	C3>D
	D17Mit46(M)	10	24.56	0.002	4.52	C<B6
D1Mit105(M)	80	161.63	0.001	8.74	C<B6	
D1Mit105(P)	80	161.63	0.001	7.81	C3>D	

Trait	Locus	position (cM)	position (10 ^{^6} bp)	p-exp	% effect	comparison
Displacement at ultimate load (VULLDS) Ultimate Load (VULLD)	D2Mit58(P)	51	109.20	0.007	3.75	C3<D
	D7Mit76(P)	3	14.04	0.018	3.29	C3<D
	D14Mit170(P)	63	97.46	0.032	2.98	C3<D
	D9Mit12(M)	55	100.44	0.020	3.34	C<B6
	D1Mit105(M)	80	161.63	0.029	3.40	C<B6
	D17Mit46(M)	10	24.56	0.023	3.36	C<B6